Published in final edited form as:
Cell Stem Cell. 2011 May 6; 8(5): 566–579. doi:10.1016/j.stem.2011.03.010.

Division-Coupled Astrocytic Differentiation and Age-Related Depletion of Neural Stem Cells in the Adult Hippocampus

Juan M. Encinas[1], **Tatyana V. Michurina**[1], **Natalia Peunova**[1], **June-Hee Park**[1], **Julie Tordo**[1], **Daniel A. Peterson**[2], **Gord Fishell**[3], **Alex Koulakov**[1], and **Grigori Enikolopov**[1]

[1]Cold Spring Harbor Laboratory, Cold Spring Harbor, NY 11724

[2]Center for Stem Cell and Regenerative Medicine and Department of Neuroscience, Rosalind Franklin University of Medicine and Science, North Chicago, IL 60064

[3]Smilow Neuroscience Program, New York University School of Medicine, New York, NY 10016

SUMMARY

Production of new neurons in the adult hippocampus decreases with age; this decline may underlie age-related cognitive impairment. Here we show that continuous depletion of the neural stem cell pool as a consequence of their division may contribute to the age-related decrease in hippocampal neurogenesis. Our results indicate that adult hippocampal stem cells, upon exiting their quiescent state, rapidly undergo a series of asymmetric divisions to produce dividing progeny destined to become neurons and subsequently convert into mature astrocytes. Thus, the decrease in the number of neural stem cells is a division-coupled process and is directly related to their production of new neurons. We present a scheme of the neurogenesis cascade in the adult hippocampus that includes a proposed “disposable stem cell” model and accounts for the disappearance of hippocampal neural stem cells, the appearance of new astrocytes, and the age-related decline in the production of new neurons.

INTRODUCTION

New neurons are continuously produced in the dentate gyrus (DG) of the hippocampus. Hippocampal neurogenesis dynamically responds to a multitude of extrinsic stimuli and may be important for cognition, behavior, pathophysiology, and brain repair, and response to therapies (Deng et al., 2010; Kempermann et al., 2004; Kriegstein and Alvarez-Buylla, 2009; Zhao et al., 2008). New neurons arise from neural stem cells, a quiescent cell population that resides in the neurogenic niche of the subgranular zone (SGZ) of the DG. Stem cells in the SGZ (described also as radial astrocytes, radial glia-like cells, Type-1 cells, and quiescent neural progenitors) (Eckenhoff and Rakic, 1984; Encinas et al., 2006; Kempermann et al., 2004; Kosaka and Hama, 1986; Kronenberg et al., 2003; Mignone et al., 2004; Seri et al., 2004; Seri et al., 2001) have astroglial characteristics under electron and light microscopy and express some markers in common with astrocytes (e.g., glial fibrillary acidic protein/GFAP and vimentin) (Kempermann et al., 2004; Kriegstein and Alvarez-

Corresponding author: Grigori Enikolopov, enik@cshl.edu, (516) 367-8316 tel, (516) 367-6805 FAX.

SUPPLEMENTAL INFORMATION Supplemental information includes 6 figures, 2 tables and Supplemental Experimental Procedures.

Buylla, 2009). They differ, however, from mature hippocampal astrocytes in their morphology, their expression profile (e.g., expressing nestin), and their ability to produce neurons.

Quiescence is one of the defining characteristics of stem cells in a range of tissues (Li and Clevers, 2010; Morrison and Spradling, 2008; Rossi et al., 2008). The conventional model of continuous self-renewal of stem cells with cyclic recurring quiescence, demonstrated most convincingly for hematopoietic stem cells, posits that a stem cell stochastically leaves the quiescent (G_0) state, undergoes an asymmetric division, and returns to a quiescent state, with the cycle repeating many times throughout the lifespan of the animal. This mode of quiescence is thought to maintain the size of the pool of stem cells while limiting their replication to reduce the probability of accumulating mutations.

Aging is associated with a continuous decline in the number of new neurons in the DG and age is the most important contributing factor to the decrease in neurogenesis in the normal brain. This decline has been reported across mammalian species, including primates (Cameron and McKay, 1999; Hattiangady and Shetty, 2008; Kuhn et al., 1996; Leuner et al., 2007; Olariu et al., 2007; Seki and Arai, 1995). Given the potential significance of new neurons for cognitive function, it has been hypothesized that reduced neurogenesis may contribute to age-related cognitive impairment (Cameron and McKay, 1999; Leuner et al., 2007). The underlying cause of this age-related decline may include an increase in neural stem cell quiescence, a decrease in their productive division or survival of their progeny, a reduction in neuronal fate commitment, or the loss of neural stem cells through death or differentiation.

Here we demonstrate that age-related decrease in hippocampal neurogenesis under normal conditions is driven by the disappearance of neural stem cells via their conversion into mature hippocampal astrocytes. Importantly, this astrocytic differentiation is coupled to a rapid succession of asymmetric divisions of the activated stem cells. Thus, in contrast to the model of multiple cycles of activation and quiescence of stem cells, hippocampal neural stem cells, once activated, leave the pool of stem cells. We describe the life cycle of an adult neural stem cell and propose a “disposable stem cell” model which reconciles the observations on the age-related decrease in production of new neurons, the age-related increase in astrocytes, the disappearance of hippocampal neural stem cells, and remodeling of the neurogenic niche; together, these continuous changes underlie age-dependent decrease in production of new neurons and may contribute to age-related cognitive impairment.

RESULTS

Stem and progenitor cells of the DG

Neural stem and progenitor cells can be readily identified in reporter mouse lines (Nestin-GFP or Nestin-CFPnuc) in which the Nestin gene regulatory elements drive the expression of fluorescent proteins (FPs) (Encinas and Enikolopov, 2008; Encinas et al., 2006; Enikolopov and Overstreet-Wadiche, 2008; Mignone et al., 2004) (Fig.1 and Fig.S1 in Supplemental Information, SI). In Nestin-based reporter lines, stem cells can be identified as radial-glia-like cells positive for GFP/CFPnuc, nestin, GFAP, brain lipid-binding protein (BLBP), and vimentin, with a long process extending from the SGZ towards the molecular layer and ramifying there. These cells reveal low level of proliferation (~1% of these cells incorporate thymidine analog 5-bromo-2-deoxyuridine, BrdU, upon pulse labeling), and therefore are defined as quiescent neural progenitors (QNPs). Another class of neural progenitors can be revealed as GFP/CFPnuc-positive round or oval cells, devoid of a long GFAP- or nestin-positive radial process, and located in the SGZ. These cells show high level of proliferation (10-20% of these cells incorporate BrdU upon pulse labeling) and are

defined as amplifying neural progenitors (ANPs). Furthermore, neural precursors are represented by neuroblasts (NBs) and young immature neurons (IN) which exit the cell cycle, cease to express the fluorescent reporter proteins and ultimately mature into granule neurons.

In addition to QNPs and ANPs, in the DG of Nestin-GFP reporter mice the transgene is expressed in NG2-positive oligodendrocyte precursor cells (OPCs) and in pericytes (Fig.1A-D). Upon short-term labeling with BrdU, the majority of labeled cells are observed in the SGZ and of those the vast majority (98%) corresponds to QNPs and ANPs (Fig.1E-G, Table S1). Labeled OPCs, pericytes, and astrocytes are present in the granule cell layer (GCL), hilus, and molecular layer of the DG; however, their absolute number is much smaller than the number of BrdU-positive QNPs and ANPs (e.g., the number of labeled astrocytes and pericytes does not exceed 0.3% and 1.1%, respectively, of all labeled cells in the DG; Figs. 1E-G and S2, Table S1). Thus, various cell subpopulations can reliably discriminated in the DG of Nestin-FP reporters.

Several lines of evidence indicate that QNPs represent the stem cell population of the DG and that ANPs, which are often observed as being separated from the soma of QNPs in an asymmetric fashion, correspond to their transit amplifying progeny (Encinas et al., 2006; Enikolopov and Overstreet-Wadiche, 2008; Mignone et al., 2004). To directly demonstrate that ANPs are born from QNPs through asymmetric divisions, we made use of genetic inducible fate mapping (GIFM). We analyzed crosses between the RCE reporter line (Balordi and Fishell, 2007) and the Gli1-CreER line, in which Cre recombinase is fused to a tamoxifen-responsive ligand-binding domain of the estrogen receptor and is expressed under the control of the Gli1 gene regulatory elements (Ahn and Joyner, 2005). In the hybrid animals, tamoxifen-induced recombination results in GFP expression in Gli1-expressing cells and their progeny. A single tamoxifen injection produced GFP-labeled QNPs detected in the SGZ as early as 12 and 24 hours after the induction, while the first labeled separated ANPs did not appear until 36 hrs post-induction (Figs.2, S3, S4). Initially, these first ANPs were in close contact with QNPs but were separate from the neighboring QNPs at later stages (Fig.2A,B). This suggests that Cre-mediated recombination first occurs in QNPs and that these GFP-labeled QNPs later give rise to ANPs. This conclusion was supported by sequential observations, 36-120 hrs after induction, of QNP/ANP pairs that completed nuclear division but have not yet separated (Fig.2C). To validate that such pairs of dividing cells were indeed at the late stages of cytokinesis (and were not merely pairs of closely positioned cells), we confirmed the presence of the midbody by immunostaining for Aurora B (Fig.2D). Similar pairs of newly-generated cells in various stages of cytokinesis were also observed in GIFM experiments with Nestin-CreER line (Balordi and Fishell, 2007) (Fig.2E) and in Nestin-GFP animals after a single pulse of BrdU (Fig.2F,H) or when immunostained for phosphorylated histone H3, a marker of dividing cells (Fig.2G,I). Importantly, while we often observed pairs and clusters of dividing ANPs (most of them indistinguishable from other cells in the cluster, suggesting a symmetric mode of division), in none of these three models have we detected pairs of dividing QNPs. These separate lines of evidence together indicate that QNPs undergo asymmetric divisions to generate ANPs.

The neural stem cell pool declines with age

We used Nestin-GFP and Nestin-CFPnuc mice to determine the age-related changes in the size of the QNPs and ANPs pools and found a dramatic decrease in both populations over time. Between three weeks and two years of age we observed a 100-fold decrease in QNPs and a 15-fold decrease in ANPs (Fig.3A-J and Table S2). The decrease in the number of QNPs was the same when QNPs were scored as GFAP-positive, nestin-positive, vimentin-positive, or BLBP-positive cells with radial morphology (Fig.3C,D,K and data not shown), indicating that this decrease is not due to an age-related reduction in transgene expression.

Unlike the total number of QNPs, the fraction of dividing cells within the QNP population did not change significantly at different ages (Fig.3L). The QNP/ANP ratio decreased over time, indicating that the age-related decrease in the number of QNPs is larger than the decrease in dividing cells (mainly represented by ANPs) (Fig.3J) and that the rate of disappearance is different for the QNPs and ANPs. Indeed, while the rate of disappearance of ANP changes only slightly throughout the lifespan of the animal and is maintained at a level of ~0.4% of cells lost every day, the rate of the QNP pool depletion changes notably over the life of the animal (Figs.3M,N and SI). While at 1 month of age 1% of QNPs disappear per day (~320 QNPs per brain), by 2 years the fraction of QNPs lost every day becomes 0.2% (~0.4 QNP per brain) and by 2.5 years (extrapolated) would reach 0.07% (Fig.3N). Thus, the QNP and ANP populations continuously decrease with age with different dynamics, with the rate of loss of QNPs significantly lower in the old, as compared to the young, brain.

Dividing stem cells disappear soon after division

We used pulse labeling experiments to track proliferation and fate of progenitor populations in the DG. Nestin-CFPnuc mice received a single injection of BrdU to label a cohort of dividing cells and the number and fraction of labeled cells in each progenitor group was analyzed over the course of 30 days. The total number of BrdU-labeled cells increased 4 fold and peaks 48 hrs after the BrdU pulse, declined to one third of the original number 10-15 days later, and stayed at that level through 30 days (Fig.4A). These results demonstrate that a substantial portion of the dividing population reenters the cell cycle; the largest observed increase in labeled cells occurs between 12 and 48 hrs, with the highest rate of increase (the rate of change per labeled cell) seen at ~20 hr (Fig.4B). Furthermore, they demonstrate that the largest loss of labeled newly-born cells is at 2-5 days, with a particularly high rate of disappearance at ~2.5-4 days; this period of rapid loss of newborn cells is followed by a prolonged period (days 7-15) of a further, slower, decrease (Fig.4B; also see (Sierra et al., 2010).

We next quantified changes in defined classes of newly-generated cells in the DG (Fig.4C-H). As expected, the number of labeled ANPs initially increased, reflecting proliferation of the ANPs and their prevalence among all labeled cells. The numbers (Fig.4C) and fractions (Fig.4D) of labeled ANPs and NBs change in a reciprocal manner indicative of a potential precursor-product relationship between these two classes. The ANP-NB transition is virtually complete after 5-7 days; at later times, the number and the fraction of NBs corresponds to those of new granule neurons, suggesting that at the later stages of maturation (15-30 days) cell loss is minimal and that the majority of surviving cells (NBs) become mature neurons. The number of BrdU-labeled QNPs did not change for 7 days and then gradually declined until none were observed 10-15 days after the BrdU pulse (this observation contrasts with the situation in the subventricular zone where labeled stem-like cells can be observed 45 days after the labeling; data not shown). Unexpectedly, detectable numbers of BrdU-labeled astrocytes (of which there were none at the start of the experiment) appeared several days after the pulse, increased to near the number of the initially labeled QNPs by 10 days, and stayed at that level until the last time point analyzed. After 30 days, the label was observed only in differentiated neurons and astrocytes, which represented 77% and 23% of the BrdU-labeled cells, respectively (Fig.4E-H). The reciprocal nature of the changes in BrdU-labeled QNPs and astrocytes and the near constancy of their sum suggest the possibility that the newly born astrocytes are derived from the dividing QNPs.

Together, the results of the pulse labeling experiment with the Nestin-CFPnuc reporter line indicate that vast majority of QNPs do not undergo symmetric divisions (the number of $BrdU^+$QNPs does not increase) but may, potentially, reenter the cell cycle through

asymmetric divisions, that ANPs reenter the cell cycle and multiply, that ANPs may convert into NBs, that most of newborn progenitors disappear, that the remaining NBs convert into granule neurons, that the decline in the number of dividing QNPs is reciprocal to the increase in new astrocytes, and that QNPs may convert into astrocytes. These results are compatible with various division/differentiation schemes, with different rates of division and loss of progenitor populations and different rates of interconversion of the populations. We used the data of the pulse-labeling experiments for the computational modeling that simulates different division/differentiation scenarios on a cell by cell basis; such modeling, rather than providing an exact description of the cascade, indicates which schemes and parameters are in best fit with the experimental data and helps to exclude those that are not compatible with the data. The results of this computational simulation (see SI for details) are an excellent fit with a scheme where the majority of ANPs undergo 2.3 divisions on average and convert into NBs which, after massive loss, convert into differentiated neurons, and where QNPs divide asymmetrically three times and, after this rapid series of divisions, convert into astrocytes.

To address the possibility that dividing QNPs convert into astrocytes, we performed a separate series of pulse labeling experiments with Nestin-GFP mice to follow the changes in the pool of BrdU-labeled $GFAP^+$Nestin-GFP^+ cells (GFAP-positive cells in the DG include both QNPs and astrocytes). Initially, the number of $BrdU^+GFAP^+$Nestin-GFP^+ cells in the SGZ and GCL (i.e., QNPs that were in S phase at the time of label injection) was the same as the number of $BrdU^+GFAP^+$ cells, but they started to diverge after 7-10 days: the number of $BrdU^+GFAP^+$Nestin-GFP^+ cells started to decrease and such cells were undetectable 20-30 days after the pulse labeling (Fig.4I-K) In contrast, although there were no BrdU-labeled astrocytes in the first 5-7 days after the labeling, by 30 days all $BrdU^+GFAP^+$ cells had the morphology of mature astrocytes (Fig.4I-J). Remarkably, the total number of $BrdU^+GFAP^+$ cells (i.e., the sum of labeled QNPs and astrocytes) did not change significantly within the entire analyzed period (Fig.4K); note that labeled QNPs do not increase in number after a pulse (Fig.4C) and that we did not observe dying QNPs (see also (Sierra et al., 2010). Thus, while initially all BrdU-labeled $GFAP^+$ cells corresponded to QNPs, subsequently all were detected as astrocytes, supporting the notion that dividing QNPs had transformed into astrocytes.

These separate pulse-labeling experiments, together with the lineage tracing experiments (Fig.2) demonstrate the progression from QNPs, through distinct phases that include progenitor amplification and massive death, to mature neurons. Our results also suggest that QNPs which entered the division cycle, rather than returning to quiescence, may engage in additional cycles of asymmetric divisions and disappear by converting into astrocytes after division.

Stem cells differentiate into astrocytes after division

To further investigate the potential astrocytic fate of QNPs, we performed a separate stem cells lineage analysis by GIFM, generating crosses between the Z/EG reporter line (Novak et al., 2000) and the Nestin-CreER line in which the CreER fusion is expressed under the control of the Nestin gene regulatory elements (Balordi and Fishell, 2007).

We first validated our Nestin-based GIFM system by analyzing the mice 24 hours and 30 days after a series of tamoxifen injections, observing GFP-labeled QNP and ANP cells (but not neurons) 24 hrs after the induction and GFP-expressing granule neurons, as well as QNPs, ANPs, and NBs, 30 days after induction (Fig.S5). Importantly, we could also detect GFP-positive astrocyte-like cells in the SGZ, GCL, hilus, and molecular layer (Fig.S5).

We then combined the genetic lineage tracing with BrdU labeling to track quantitatively and qualitatively the fate of specific cohorts of dividing cells, focusing on GFAP-expressing $BrdU^+GFP^+$ cells (Fig.5). The number of $BrdU^+GFP^+GFAP^+$ cells (marking both QNPs and astrocytes, Fig.5A,B), did not change significantly from 10 to 45 days upon 5 days of tamoxifen induction and accounted for ~15% of newborn GFP^+ cells, Likewise, the number of newly-generated neurons ($BrdU^+GFP^+NeuN^+$ cells, encompassing young and mature new neurons) did not change within this period and accounted for ~85% of newborn GFP^+ cells (Fig.5C,E), similarly to the results with Nestin-CFPnuc and Nestin-GFP mice. In contrast, newly-generated mature astrocytes ($BrdU^+GFP^+S100\beta^+$ cells) were not detected until 20 days post induction but by 45 days accounted for ~15% of the newborn GFP^+ cells (Fig.5D, E). Thus, separate lines of evidence (pulse labeling experiments with Nestin-CFPnuc mice, Fig.4A-H, with Nestin-GFP mice, Fig.4I-K, and present results, Fig.5) suggest that the DG stem cells generate both mature neurons and mature astrocytes after division.

This conclusion was further supported by assessing the morphology of newly generated genetically labeled ($BrdU^+GFP^+$) cells (Fig.5 and Fig.S5). $BrdU^+GFP^+GFAP^+$ QNP cells evidenced a systematic morphological progression from a single radial apical process at day 1 after tamoxifen induction to branching apical process at day 5, to further branching of the process and short cytoplasmic prolongations (10-20μm) emerging from the basal area of the cells' soma at day 7, to further complex apical branching with more extensive basal extensions (>30μm) and soma migration away from the SGZ at day 10 (Figs.5A, S5). Fifteen days after induction, cells with apical, basal, and lateral branching processes with multiple ramifications appeared. Finally, by 30-45 days, $BrdU^+GFP^+GFAP^+$ cells with characteristic star-shape morphology and extensive ramification of the branches were observed in the GCL, hilus, and molecular layer (Figs.5B,D, S5). These cells also expressed S100β and were indistinguishable from the surrounding astrocytes. Notably, the proportion of neurons (84.5%) and astrocytes (14.5%) among $BrdU^+GFP^+$ cells after 45 days (Fig.5E) was similar to that seen with BrdU labeling (Fig.4C), further confirming the validity of the genetic labeling method.

The migration of new astrocytes was mainly outward, with most of them found at first in the SGZ and the GCL with a few in the hilus very close to the SGZ. Later most of the new astrocytes (85%) were found in the upper layers of the GCL, with a small fraction (~5%) reaching the molecular layer at the late time points, and another fraction (~10%) located in the hilus close to the SGZ (Figs.5A,B,D, S5F-H, S6). This was observed in all three transgenic mouse lines that we tested – Nestin-GFP, Nestin-CFPnuc, and Nestin-CreER/Z/EG.

We next examined whether newly-formed astrocytes divide, by injecting nucleotide analogs (BrdU or ethynyl deoxyuridine, EdU) to Nestin-CreER/Z/EG or Nestin-CreER/RCE animals 2 or 8 months after the tamoxifen induction (although we do not observe labeled astrocytes in the SGZ and GCL after pulse labeling, Figs.1, 4, it is conceivable that newborn astrocytes, themselves a small fraction, are enriched in dividing cells). We did not observe any BrdU- or EdU-labeled GFP^+GFAP^+ astrocytes, indicating that under normal conditions QNP-derived astrocytes do not reenter the cell cycle.

Together, the pulse- and genetic labeling experiments indicate that stem cells of the DG convert into astrocytes (schematically presented in Fig.5F). Furthermore, they indicate that astrocytic differentiation of QNPs is coupled to their division.

Mitotic potential of stem and progenitor cells

To analyze division of QNPs and ANPs with better temporal resolution, we utilized sequential thymidine analog labeling with 5-chloro-2-deoxyuridine (CldU) and 5-iodo-2-

deoxyuridine (IdU) (Vega and Peterson, 2005) (Fig.6A). Nestin-GFP mice were injected with CldU to define an initial proliferative cohort and, at different time intervals (0-20 days), with IdU to mark cells which pass through the same or a subsequent S phase (Fig.6A-C). By determining the fraction of CldU/IdU double-labeled QNP and ANP cells, it is possible to track the progression of a progenitor cohort through the rounds of proliferation and to determine the number of divisions, the length of S phase, and the length of the division cycle for each class.

When CldU and IdU nucleotides were injected simultaneously, all IdU-labeled ANP cells were co-labeled with CldU. After that the fraction of double-labeled cells decreased because some of the cells labeled by CldU have left S phase by the time of the IdU injection. The rate of this initial decrease allows determining the length of the S phase (Hayes and Nowakowski, 2002) as 12.2+/-1.1 hr for the ANPs and 7.8+/-0.7 hr for QNPs (see SI for details). For the ANPs, a second peak of double labeling (63% of the IdU-positive ANP cohort also labeled with CldU) was observed at the t=28 hr between label injections (Fig. 6D), indicating that the majority of those ANPs that were in S phase at the time of CldU labeling, underwent a second round of division. A third peak of double labeling was seen at the t=70 hr after the first division, indicating that a large fraction of cells (48% of the initial ANP cohort) had entered a third round of division. A small fraction of double labeled ANP (17% of the cohort) was also seen at 120 hrs, suggesting a fourth round of division for a subpopulation of ANPs; no further peaks were detected 7, 10, 15, or 20 days after the initial CldU labeling. The first division (marked by CldU incorporation) reflects both the ANP cells that are born from QNP cells through asymmetric division and the ANP cells undergoing further rounds of divisions. Thus, these results indicate that once ANPs are born from QNPs, most undergo two rounds of divisions before exiting the cell cycle, with a fraction undergoing 3 rounds, on average.

The lengths of the S phases for the ANPs and QNPs and the ratio of labeled ANPs to labeled QNPs after short term labeling can then be used to estimate the number of divisions that ANPs undergo as 2.45 (see SI for details; importantly, this approach relies on the results obtained shortly after label injection and therefore is not affected by potential dilution of the label after numerous division cycles). This value is close to the independently derived results of the computational simulation of a separate dataset (2.3 divisions of ANPs, single label pulse experiment, Fig.4) and the number of peaks of ANP divisions in the double label experiments above (Fig.6D).

Remarkably, we could also detect several rounds of division of QNPs predicted by the computational simulation of the single label pulse experiment (Fig.6D); as with ANPs, no further double labeled cells were detected 7-20 days after the initial labeling. Importantly, the number of CldU-labeled QNP cells did not change significantly for at least 7 days (paralleling the results of the single label pulse experiments in Fig.4K), indicating that the decrease in the fraction of double-labeled cells is not due to the dilution of label. Also note that the CldU injection labels populations of cells which are in their first, second, or third round of division; therefore, if each QNP cell undergoes three divisions, ~2/3 of the initially labeled cohort is expected to be double-labeled at the time of the second division, close to the observed values. Thus, these experiments indicate that the majority of QNPs that have divided once, within a day enter a second and then a third round of division.

The conclusion that QNPs rapidly reenter the cell cycle after their activation and division contrasts with the notion of prolonged periods of quiescence between stem cell divisions. Confirming our conclusions, we observed numerous clusters containing several BrdU-labeled ANPs next to a BrdU-labeled QNP after a pulse 2hr labeling (Fig.6E), corresponding to ANPs in S phase next to a QNP from which they were derived and which has reentered

the S phase; such clusters should not be observed if a QNP becomes quiescent after giving birth to an ANP (which then undergoes rounds of division). The results of the double-label pulse experiment, taken together with the results of the single-label pulse experiment (Fig.4) and lineage analysis (Fig.5), suggest that under normal conditions QNPs, once activated, undergo a rapid succession of divisions, exit the cycle, and convert into astrocytes.

Division/differentiation scheme of adult hippocampal neurogenesis

Our results allow us to define the normal outcome of hippocampal stem cell activation and to describe a novel division/differentiation diagram for hippocampal neurogenesis (Fig.7A). Each of the stages and cell types can be identified by the expression of reporters and markers, morphology, and mitotic activity. Our data suggest that QNPs correspond to the stem cell population of the adult DG and give rise to both neurons (indirectly, through intermediate ANP daughter cells) and astrocytes (directly, through differentiation). Our results are best described by a scheme where QNPs, once activated, enter the division cycle to generate, through asymmetric divisions, the ANPs that, after ~2 rounds of symmetric divisions, exit the cell cycle and become postmitotic NB1 cells, with the majority of the newborn cells getting eliminated. The remaining NB1 cells mature into NB2 and then IN and then differentiated mature neurons. Immediately after giving rise to a daughter ANP cell, the activated QNP enters another division cycle, with the daughter ANP following the pathway of the previous ANP. After a rapid succession of ~3 divisions, QNPs exit the cell cycle and start acquiring the astrocytic morphology (note that the numbers of division rounds for ANPs and QNPs presented here refer to a young adult mouse and the results in Fig.3 indicate that these numbers may change with age). This scheme predicts particular combinations of labeled ANPs and QNPs at different rounds of division and, indeed, we were able to observe each of the predicted combinations after short-term labeling (Fig.7B), further validating the model.

DISCUSSION

Disposable stem cells

Our results provide evidence for a new model for the regulation of stem cells and for their contribution to neurogenesis and astrogenesis in the adult hippocampus. Furthermore, they indicate that continuous decrease in the number of neural stem cells underlies the age-related decline in hippocampal neurogenesis.

Our results, by demonstrating that activation of stem cells eventually leads to their conversion into astrocytes, imply that under normal conditions hippocampal stem cells are used only once in the adult life and, while physically present in the DG, withdraw from the stem cell pool after a rapid series of divisions. These results support a model in which a stem cell of the adult brain can be described as a “single use” or a “disposable” unit: quiescent for the entirety of its adult lifetime, activated to undergo a series of rapid asymmetric divisions (with progeny, after additional divisions and massive elimination, maturing into neurons) and then, via differentiation into an astrocyte, abandoned in its capacity to act as a bona fide stem cell. This “disposable stem cell” model, presented schematically in Fig.7C, links together the age-related decrease in hippocampal neural stem cells, decrease in new neurons, and increase in astrocytes. Furthermore, it indicates that disappearance of hippocampal stem cells is directly linked to production of new neurons and new astrocytes.

This “disposable stem cell” model contrasts with the conventional model of repeated self-renewal of stem cells followed by periods of quiescence (Fig.7C). A prototypical example of the latter model is hematopoietic stem cells, which leave the quiescent pool every several weeks, divide, and return to G_0 to be activated again at later times (Kiel et al., 2007).

Importantly, the number of hematopoietic stem cells does not decline with age (Morrison and Spradling, 2008; Rossi et al., 2008). This “cyclic recurring quiescence” model may be also pertinent to other tissues that do not exhibit age-related decline in the number of stem cells. In contrast, the “disposable stem cell” model may be employed by tissues in which production of differentiated cells declines with age.

Our analysis focuses on QNPs, a population of cells defined by their characteristic morphology, low mitotic activity, and expression of the Nestin-driven reporter transgenes. QNPs encompass the majority of neuron-producing stem cell activity in the adult DG and overlap to a large degree with other varieties of hippocampal stem cells which have been identified structurally, functionally, or by expression of other reporters (Eckenhoff and Rakic, 1984; Garcia et al., 2004; Kosaka and Hama, 1986; Kronenberg et al., 2003; Lugert et al., 2010; Seri et al., 2001; Suh et al., 2007). However, our results do not exclude possibilities that DG contains small populations of Nestin-FP-expressing stem cells with repeated self renewal, stem cells with unusually long G2/M phases, or stem cells which are not detected using Nestin-driven reporter systems (Li and Clevers, 2010; Suh et al., 2007; Zhao et al., 2008). Such populations, however, would represent a significantly smaller fraction of the stem cell pool than the “disposable” Nestin-FP-expressing population, although their contribution may increase upon trauma or physiological demand (Li and Clevers, 2010). Also note that while we do not observe division of newly-derived astrocytes, our model does not preclude the possibility that under specific conditions, e.g., trauma or disease, such astrocytes may be recruited to contribute again to the stem cell pool.

The conversion of adult neural stem cells into astrocytes may have the dual consequence of depleting the pool of precursors while continuously remodeling the neurogenic niche in the DG. In contrast to new neurons, the number of hippocampal astrocytes increases with age (Mouton et al., 2002; Pilegaard and Ladefoged, 1996); furthermore, they have an instructive role in adult neurogenesis through promotion of neuronal differentiation and integration of young neurons (Song et al., 2002). Thus, it is conceivable that by converting into astrocytes, former stem cells contribute to the neuronal differentiation of their or their neighbors’ progeny. Furthermore, new astrocytes may affect the remaining stem cells by influencing their rate of activation and helping to preserve the stem cell pool in the aging brain.

The conversion of QNPs from radial-glia like cells into astrocytes bears formal resemblance to the process of astrocyte generation in the embryonic and perinatal forebrain (Kriegstein and Alvarez-Buylla, 2009); however, whereas this conversion takes several days during development, it might be extended over many months in the adult hippocampus and includes a prolonged period of quiescence.

Division and differentiation cascade in the DG

Our results describe the details of cell division and differentiation in the adult hippocampus and provide a comprehensive scheme of the neurogenic and astrogenic arms of the cascade. Together with the computational model for evaluating stem cell dynamics, this detailed description of hippocampal stem cell life cycle provides a conceptual framework with which to map the targets of various neurogenic stimuli and compare different strategies by which stem cells are harnessed for tissue regeneration.

We applied several non-overlapping approaches (single- and double-nucleotide pulse labeling, lineage tracing, and computational modeling) which provided remarkably similar estimates of the parameters of the cascade. For instance, the number of divisions of ANPs is determined as 2.45 from the ratio of labeled ANPs to QNPs after a short labeling period, as 2.3 from the computational simulation of the single label pulse experiment (Fig.4); and as ~2 using sequential double-labeling paradigm (number of detectable peaks of double-labeled

cells; Fig.6); the number of divisions of QNPs is determined as 3 from the computational simulation, as 3 from the number of detectable peaks of double-labeled cells, and as 3 using the height of the second peak in the same experiment (also see SI) (note, however, that these values reflect the average behavior of the QNP and ANP populations). These close values serve to increase the confidence in the results and validate the approaches we used to analyze the cascade.

These independently derived parameters of the cascade provide additional support for our "disposable stem cell" model, through the comparison of the rate at which QNPs are activated (enter a series of divisions) and the rate of their disappearance. According to the model, which proposes division-coupled astrocytic differentiation of QNPs as the main reason for their decline, the rates of QNP activation and disappearance have to match closely. Indeed, using non-overlapping approaches to determine these two parameters, we found that under normal conditions an approximate balance exists between QNP activation and QNP disappearance from the stem cell pool (~150 QNP cells are activated and ~170 QNPs disappear each day; see SI for details). The remarkable similarity of these independently derived rates of division and disappearance further supports the conclusion that hippocampal stem cells, after entering the rounds of division, exit the stem cell pool by converting into astrocytes and that the age-dependent loss of stem cells occurs in a use-dependent manner.

An important consideration in the nucleotide labeling experiments is the potential dilution of the label below the level of detection due to consecutive divisions. Our results present several independent lines of evidence that our conclusions are not compromised by the potential dilution of the CldU or BrdU label below the level of detection. Briefly, (a) periods of QNP division and their disappearance in double-label pulse experiments (Fig.6) do not overlap and are significantly separated in time and therefore the observed loss of labeled QNPs is not explained by the label dilution; (b) ~90% of the initially labeled QNPs can be accounted for 30 days after labeling (Figs.4B,J) and the number of $BrdU^+GFAP^+$ cells is sustained over this time, further indicating that the impact of the label dilution on our conclusions is negligible; (c) numbers of the QNP and ANP divisions determined within several hours after label injection are in excellent agreement with the independently derived results of long-term labeling experiments, again arguing against the distortion of the results by the potential label dilution (additional discussion is presented in the SI). Note that the situation may be different in other contexts, e.g., if there are so many divisions that the label is diluted beyond the level of detection. In such cases, one should apply approaches which rely on data collected soon after label injection and which are thus not compromised by the potential dilution of the label (e.g., the ratio of BrdU-labeled ANPs to BrdU-labeled QNPs in the single-label experiment or the value of the second peak in the double-label experiments).

Age-related decrease in neural stem cells

Aging is accompanied by a continuous decrease in the regenerative capacity of many organs (Morrison and Spradling, 2008; Rossi et al., 2008). For the brain, this decrease may underlie age-related cognitive decline and limit plasticity and repair. In the hippocampus, age-related reduction of neurogenesis is observed in humans and in laboratory and wild-living mammals. The mechanisms underlying the diminished production of new granule neurons in the hippocampus are not understood and may be driven by a host of different processes, including a decrease of size of the neural stem cell pool, diminished proliferative capacity of stem cells or their progeny, reduced survival of stem cells or their progeny, or reduced neuronal lineage commitment. Our results indicate that the division-coupled conversion of neural stem cells into mature astrocytes and, therefore, continuous decrease of the pool of stem cells may be a fundamental cause of age-related decline in hippocampal neurogenesis.

Note, however, that since only a small fraction of stem cells is activated for division at different ages, the pool of stem cells and the number of new neurons they produce, while in continuous decline, does not come to a halt in older animals and can be further increased by appropriate stimuli (Cameron and McKay, 1999). Of importance, most of the factors that increase neurogenesis, e.g., fluoxetine, exercise, and deep brain stimulation (Encinas et al., 2011; Encinas et al., 2006; Hodge et al., 2008) act downstream of stem cells, at the level of ANPs and NBs, leaving the pool of stem cells unaffected. In contrast, trauma, seizures, and disease activate stem cell division (Gao et al., 2009; Huttmann et al., 2003; Park and Enikolopov, 2010; Segi-Nishida et al., 2008) and may contribute to their accelerated loss.

An important implication from our results is that the disappearance of neural stem cell is a direct consequence of them producing new neurons and that the decline of the stem cell pool may be the price paid for being able to produce new neurons as adults. At the same time, as suggested by our results, the hippocampus, while becoming more frugal in its usage of stem cells with age (with the rate of neural stem cell attrition in the hippocampus decreasing up to 10-fold with age, Fig.3), also manages to generate more dividing cells from each stem cell, such that the age-related loss in new neurons in the DG is significantly less than the loss in stem cells. It remains to be determined if this is accomplished by additional divisions of QNPs or ANPs, or reduced death of NBs; note that our results showing that the QNP/ANP ratio changes with age (Fig.3), point to an increased productivity of stem cells in the aging brain. Together, the decreased rate of hippocampal stem cell activation and disappearance, their increased output, and the continuous astrocyte-mediated remodeling of the niche by former stem cells may constitute a complex strategy for supporting neurogenesis in the aging hippocampus in the face of an ever-diminishing pool of stem cells.

EXPERIMENTAL PROCEDURES

Animals

All experiments were performed using C57B6 mice and Nestin-GFP (Mignone et al., 2004), and Nestin-CFPnuc (Encinas et al., 2006) transgenic mice. Nestin-GFP and Nestin-CFPnuc were crossed to C57B6 mice for at least 10 generations. Z/EG [Tg(ACTB-Bgeo/GFP)21Lbe] reporter mice (Novak et al., 2000) were obtained from The Jackson Laboratory. Rosa26/CMV-loxP-stop-loxP-GFP (RCE) and Nestin-CreER mice were generated by G.F. (Balordi and Fishell, 2007). Gli1-CreER mice were generated by Joyner and collaborators (Ahn and Joyner, 2005). The age and number of animals are indicated in the figure legends and the figures, with each animal represented by a dot on the graph. Use of animals was reviewed and approved by the CSHL Animal Care and Use Committee.

Lineage analysis was performed as described (Ahn and Joyner, 2005; Balordi and Fishell, 2007), with additional details presented in Supplemental Information.

Immunocytochemistry, image capture and quantification were performed following optimized previously described procedures (Encinas and Enikolopov, 2008; Encinas et al., 2011; Encinas et al., 2006) and are described in detail in Supplemental Information.

Computational modeling and processing of the experimental data are described in Supplemental Information.

Supplementary Material

Refer to Web version on PubMed Central for supplementary material.

Acknowledgments

We thank Ali Krimmer for help with experiments, Alex Joyner (MSKCC) for the Gli1-CreER line, Jayshree Samanta (NYU) for animals, Yuri Lazebnik and Bill Earnshaw for advice, and Amanda Sierra (BCM) and Julian Banerji (MGH) for insightful discussions and comments. JME is a recipient of a Young Investigator Award from NARSAD. This work was supported by grants from the National Institutes of Health: from NIA to D.A.P., from NICHD to G.F., from NINDS and NIMH to G.E.; and from NARSAD, NYSTEM, the Ira Hazan Fund, and The Ellison Medical Foundation to G.E.

References

Ahn S, Joyner AL. In vivo analysis of quiescent adult neural stem cells responding to Sonic hedgehog. Nature. 2005; 437:894–897. [PubMed: 16208373]

Balordi F, Fishell G. Mosaic removal of hedgehog signaling in the adult SVZ reveals that the residual wild-type stem cells have a limited capacity for self-renewal. J Neurosci. 2007; 27:14248–14259. [PubMed: 18160632]

Cameron HA, McKay RD. Restoring production of hippocampal neurons in old age. Nat Neurosci. 1999; 2:894–897. [PubMed: 10491610]

Deng W, Aimone JB, Gage FH. New neurons and new memories: how does adult hippocampal neurogenesis affect learning and memory? Nat Rev Neurosci. 2010; 11:339–350. [PubMed: 20354534]

Eckenhoff MMF, Rakic PP. Radial organization of the hippocampal dentate gyrus: a Golgi, ultrastructural, and immunocytochemical analysis in the developing rhesus monkey. Journal of comparative neurology. 1984; 223:1–21. [PubMed: 6707248]

Encinas JM, Enikolopov G. Identifying and quantitating neural stem and progenitor cells in the adult brain. Methods Cell Biol. 2008; 85:243–272. [PubMed: 18155466]

Encinas JM, Hamani C, Lozano AM, Enikolopov G. Neurogenic hippocampal targets of deep brain stimulation. J Comp Neurol. 2011; 519:6–20. [PubMed: 21120924]

Encinas JM, Vaahtokari A, Enikolopov G. Fluoxetine targets early progenitor cells in the adult brain. Proc Natl Acad Sci U S A. 2006; 103:8233–8238. [PubMed: 16702546]

Enikolopov, G.; Overstreet-Wadiche, L. Transgenic reporter lines for studying adult neurogenesis. In: Gage, GKF.; Song, H., editors. Adult Neurogenesis. CSHL Press; 2008.

Gao X, Enikolopov G, Chen J. Moderate traumatic brain injury promotes proliferation of quiescent neural progenitors in the adult hippocampus. Exp Neurol. 2009

Garcia AD, Doan NB, Imura T, Bush TG, Sofroniew MV. GFAP-expressing progenitors are the principal source of constitutive neurogenesis in adult mouse forebrain. Nat Neurosci. 2004; 7:1233–1241. [PubMed: 15494728]

Hattiangady B, Shetty AK. Aging does not alter the number or phenotype of putative stem/progenitor cells in the neurogenic region of the hippocampus. Neurobiol Aging. 2008; 29:129–147. [PubMed: 17092610]

Hayes NL, Nowakowski RS. Dynamics of cell proliferation in the adult dentate gyrus of two inbred strains of mice. Brain Res Dev Brain Res. 2002; 134:77–85.

Hodge RD, Kowalczyk TD, Wolf SA, Encinas JM, Rippey C, Enikolopov G, Kempermann G, Hevner RF. Intermediate progenitors in adult hippocampal neurogenesis: Tbr2 expression and coordinate regulation of neuronal output. J Neurosci. 2008; 28:3707–3717. [PubMed: 18385329]

Huttmann K, Sadgrove M, Wallraff A, Hinterkeuser S, Kirchhoff F, Steinhauser C, Gray WP. Seizures preferentially stimulate proliferation of radial glia-like astrocytes in the adult dentate gyrus: functional and immunocytochemical analysis. Eur J Neurosci. 2003; 18:2769–2778. [PubMed: 14656326]

Kempermann G, Jessberger S, Steiner B, Kronenberg G. Milestones of neuronal development in the adult hippocampus. Trends Neurosci. 2004; 27:447–452. [PubMed: 15271491]

Kiel MJ, He S, Ashkenazi R, Gentry SN, Teta M, Kushner JA, Jackson TL, Morrison SJ. Haematopoietic stem cells do not asymmetrically segregate chromosomes or retain BrdU. Nature. 2007; 449:238–242. [PubMed: 17728714]

Kosaka T, Hama K. Three-dimensional structure of astrocytes in the rat dentate gyrus. J Comp Neurol. 1986; 249:242–260. [PubMed: 3525618]

Kriegstein A, Alvarez-Buylla A. The glial nature of embryonic and adult neural stem cells. Annu Rev Neurosci. 2009; 32:149–184. [PubMed: 19555289]

Kronenberg G, Reuter K, Steiner B, Brandt MD, Jessberger S, Yamaguchi M, Kempermann G. Subpopulations of proliferating cells of the adult hippocampus respond differently to physiologic neurogenic stimuli. J Comp Neurol. 2003; 467:455–463. [PubMed: 14624480]

Kuhn HG, Dickinson-Anson H, Gage FH. Neurogenesis in the dentate gyrus of the adult rat: age-related decrease of neuronal progenitor proliferation. J Neurosci. 1996; 16:2027–2033. [PubMed: 8604047]

Leuner B, Kozorovitskiy Y, Gross CG, Gould E. Diminished adult neurogenesis in the marmoset brain precedes old age. Proc Natl Acad Sci U S A. 2007; 104:17169–17173. [PubMed: 17940008]

Li L, Clevers H. Coexistence of quiescent and active adult stem cells in mammals. Science. 2010; 327:542–545. [PubMed: 20110496]

Lugert S, Basak O, Knuckles P, Haussler U, Fabel K, Gotz M, Haas CA, Kempermann G, Taylor V, Giachino C. Quiescent and active hippocampal neural stem cells with distinct morphologies respond selectively to physiological and pathological stimuli and aging. Cell Stem Cell. 2010; 6:445–456. [PubMed: 20452319]

Mignone JL, Kukekov V, Chiang AS, Steindler D, Enikolopov G. Neural stem and progenitor cells in nestin-GFP transgenic mice. J Comp Neurol. 2004; 469:311–324. [PubMed: 14730584]

Morrison SJ, Spradling AC. Stem cells and niches: mechanisms that promote stem cell maintenance throughout life. Cell. 2008; 132:598–611. [PubMed: 18295578]

Mouton PR, Long JM, Lei DL, Howard V, Jucker M, Calhoun ME, Ingram DK. Age and gender effects on microglia and astrocyte numbers in brains of mice. Brain Res. 2002; 956:30–35. [PubMed: 12426043]

Novak A, Guo C, Yang W, Nagy A, Lobe CG. Z/EG, a double reporter mouse line that expresses enhanced green fluorescent protein upon Cre-mediated excision. Genesis. 2000; 28:147–155. [PubMed: 11105057]

Olariu A, Cleaver KM, Cameron HA. Decreased neurogenesis in aged rats results from loss of granule cell precursors without lengthening of the cell cycle. J Comp Neurol. 2007; 501:659–667. [PubMed: 17278139]

Park JH, Enikolopov G. Transient elevation of adult hippocampal neurogenesis after dopamine depletion. Exp Neurol. 2010; 222:267–276. [PubMed: 20079351]

Pilegaard K, Ladefoged O. Total number of astrocytes in the molecular layer of the dentate gyrus of rats at different ages. Anal Quant Cytol Histol. 1996; 18:279–285. [PubMed: 8862669]

Rossi DJ, Jamieson CH, Weissman IL. Stems cells and the pathways to aging and cancer. Cell. 2008; 132:681–696. [PubMed: 18295583]

Segi-Nishida E, Warner-Schmidt JL, Duman RS. Electroconvulsive seizure and VEGF increase the proliferation of neural stem-like cells in rat hippocampus. Proc Natl Acad Sci U S A. 2008; 105:11352–11357. [PubMed: 18682560]

Seki T, Arai Y. Age-related production of new granule cells in the adult dentate gyrus. Neuroreport. 1995; 6:2479–2482. [PubMed: 8741746]

Seri B, Garcia-Verdugo JM, Collado-Morente L, McEwen BS, Alvarez-Buylla A. Cell types, lineage, and architecture of the germinal zone in the adult dentate gyrus. J Comp Neurol. 2004; 478:359–378. [PubMed: 15384070]

Seri B, Garcia-Verdugo JM, McEwen BS, Alvarez-Buylla A. Astrocytes give rise to new neurons in the adult mammalian hippocampus. J Neurosci. 2001; 21:7153–7160. [PubMed: 11549726]

Sierra A, Encinas JM, Deudero JJ, Chancey JH, Enikolopov G, Overstreet-Wadiche LS, Tsirka SE, Maletic-Savatic M. Microglia Shape Adult Hippocampal Neurogenesis through Apoptosis-Coupled Phagocytosis. Cell Stem Cell. 2010; 7:483–495. [PubMed: 20887954]

Song H, Stevens CF, Gage FH. Astroglia induce neurogenesis from adult neural stem cells. Nature. 2002; 417:39–44. [PubMed: 11986659]

Suh H, Consiglio A, Ray J, Sawai T, D'Amour KA, Gage FH. In vivo fate analysis reveals the multipotent and self-renewal capacities of Sox2+ neural stem cells in the adult hippocampus. Cell Stem Cell. 2007; 1:515–528. [PubMed: 18371391]

Vega CJ, Peterson DA. Stem cell proliferative history in tissue revealed by temporal halogenated thymidine analog discrimination. Nature methods. 2005; 2:167–169. [PubMed: 15782184]

Zhao C, Deng W, Gage FH. Mechanisms and functional implications of adult neurogenesis. Cell. 2008; 132:645–660. [PubMed: 18295581]

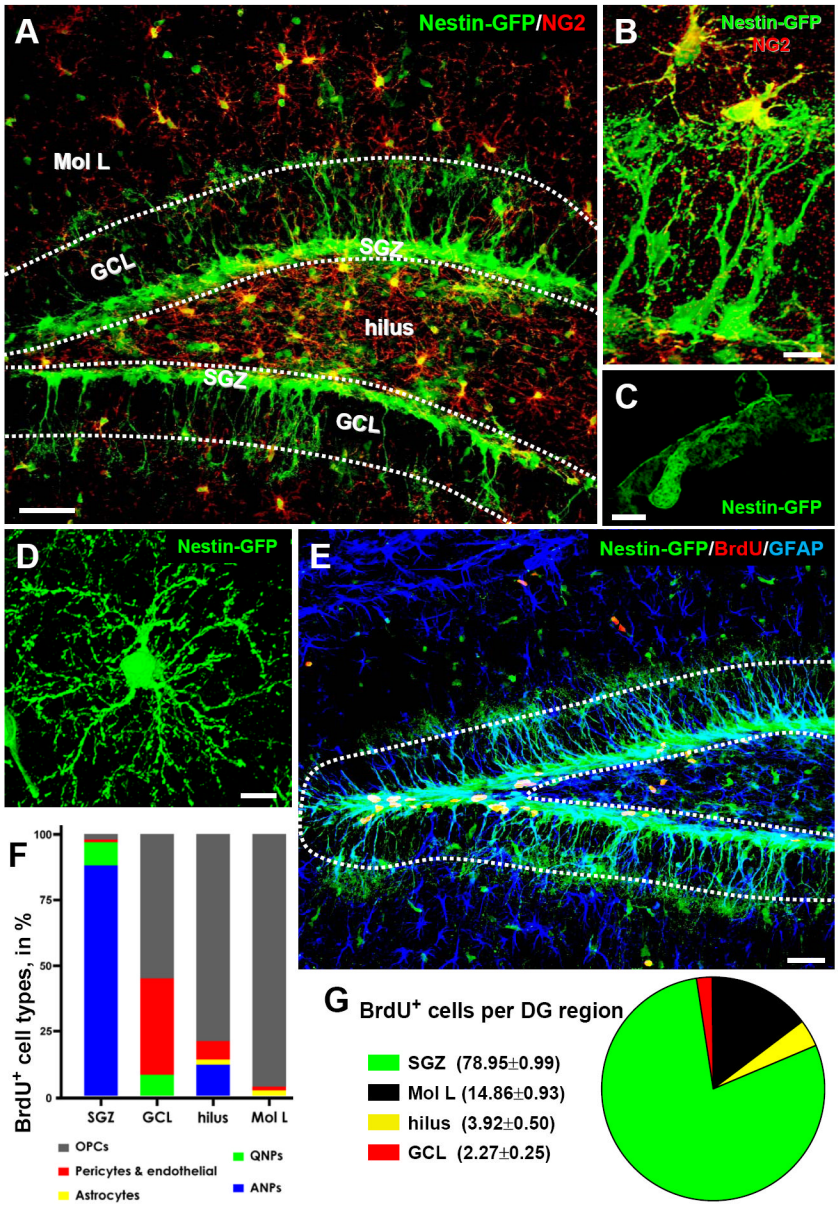

Fig. 1. Nestin-GFP expressing cells and dividing cell populations in the DG

(A, B) Distribution of Nestin-GFP-expressing cells in the DG, after immunostaining for GFP (green) and NG2 (red). Pericytes and oligodendrocyte progenitor cells (OPCs, immunopositive for NG2), are distributed throughout the DG, but are largely excluded from the GCL and the SGZ (outlined).

(C, D) High magnification images of a pericyte **(C)** and an OPC **(D)**.

(E-G). Dividing cells in the DG. Nestin-GFP mice (n=4; age 2 months) received 3 injections of BrdU (150mg/kg) at 3 hr intervals and were sacrificed 1hr after the last injection. The number and phenotype of BrdU-positive cells (red) was determined, after staining for GFP (green) and GFAP (blue), for the defined regions of the DG: molecular layer (Mol L), GCL, SGZ, and hilus. Vast majority of dividing cells are located in the SGZ. Outside the SGZ, where QNPs and ANPs account for the largest number of dividing cells, NG2-positive morphologically distinct OPCs are the main proliferating cell type. In rare occasions, $BrdU^+Nestin\text{-}GFP^+$ pericytes and $BrdU^+Nestin\text{-}GFP^-$ cells (most likely representing

endothelial cells) were detected in the blood vessels. Extremely rare $BrdU^{+}GFAP^{+}Nestin\text{-}GFP^{-}$ astrocytes were observed only in the hilus and the molecular layer.
Scale bars are 50μm in **A**, 10μm in **B**, 5μm in **C** and **D**., and 75μm in **E**.
See also Figures S1 and S2 and Table S1.

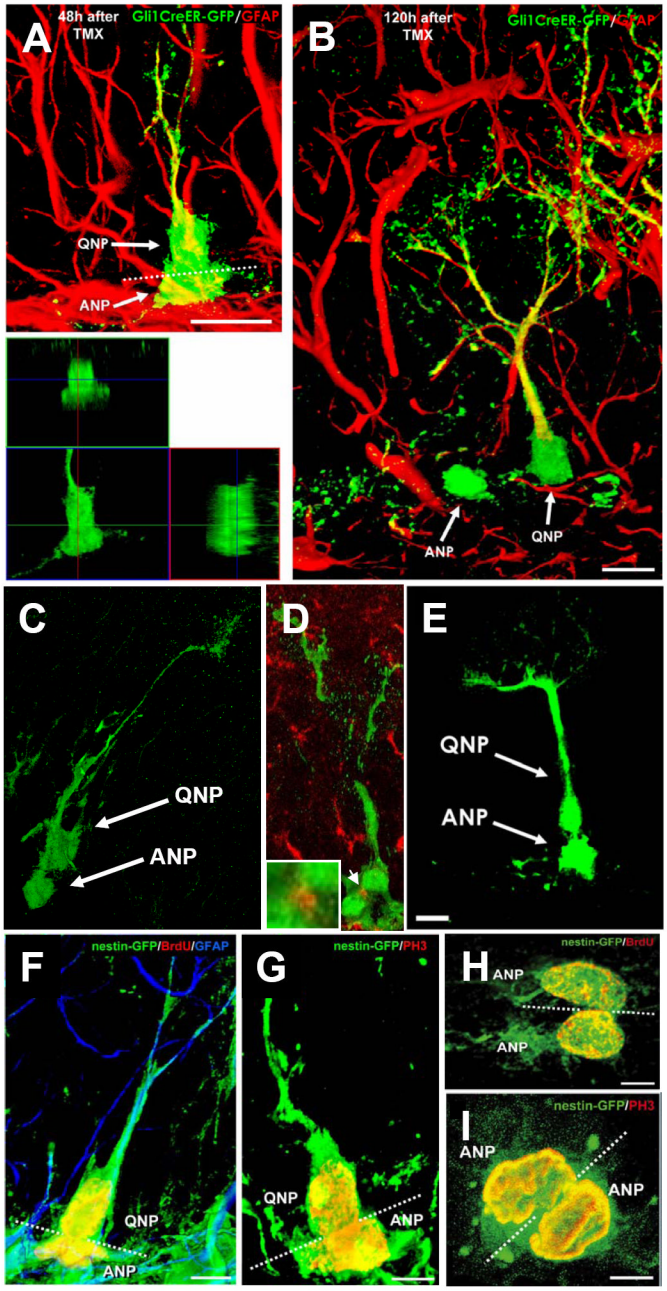

Fig. 2. ANPs are born from QNPs

(A,B) In Gli1-CreER/RCE animals, GFP is expressed exclusively in QNPs 12-18 hr after tamoxifen induction. Later (48 hr after the induction in A), asymmetrically dividing QNPs giving rise to ANPs can be observed; lower panel shows a focal plane from the orthogonal projection of the same pair of cells. Plane of division (dotted line) is often parallel to the SGZ. Furthermore (120 hr after the induction in B), separate ANPs can be identified.

(C, D) A pair of QNP and ANP cells in late telophase in the DG of Gli1-CreER/RCE mouse 24 hrs after tamoxifen induction. In D, the midbody is visualized by antibody to Aurora B (arrow; also shown at higher magnification in the inset) to show that such pairs indeed correspond to a newly divided QNP and its daughter cell.

(E) A pair of a QNP and an ANP cell in late telophase in the DG of Nestin-CreER/Z/EG mouse 24 hr after tamoxifen induction.
(F-I) Pairs of QNP and ANP cells **(F, G)** and of ANP cells **(H, I)** in telophase in the DG of Nestin-GFP mice; **F** and **I** are z-stack maximum projections (5 and 7μm thick, respectively), **G** and **H** are single focal planes (1μm thick). Nuclei of dividing cells are visualized with antibodies to BrdU (24 hr after a single pulse) **(F, H)** or to phosphorylated histone H3 **(G, I)**. The plane of division (dotted line) is most often parallel to the SGZ for the QNP/ANP pairs but can be different for the ANP pairs. Channels for multiple labels are indicated on the figures. Scale bar is 10μm in A-E and 5μm in F-I.
See also Figures S3 and S4.

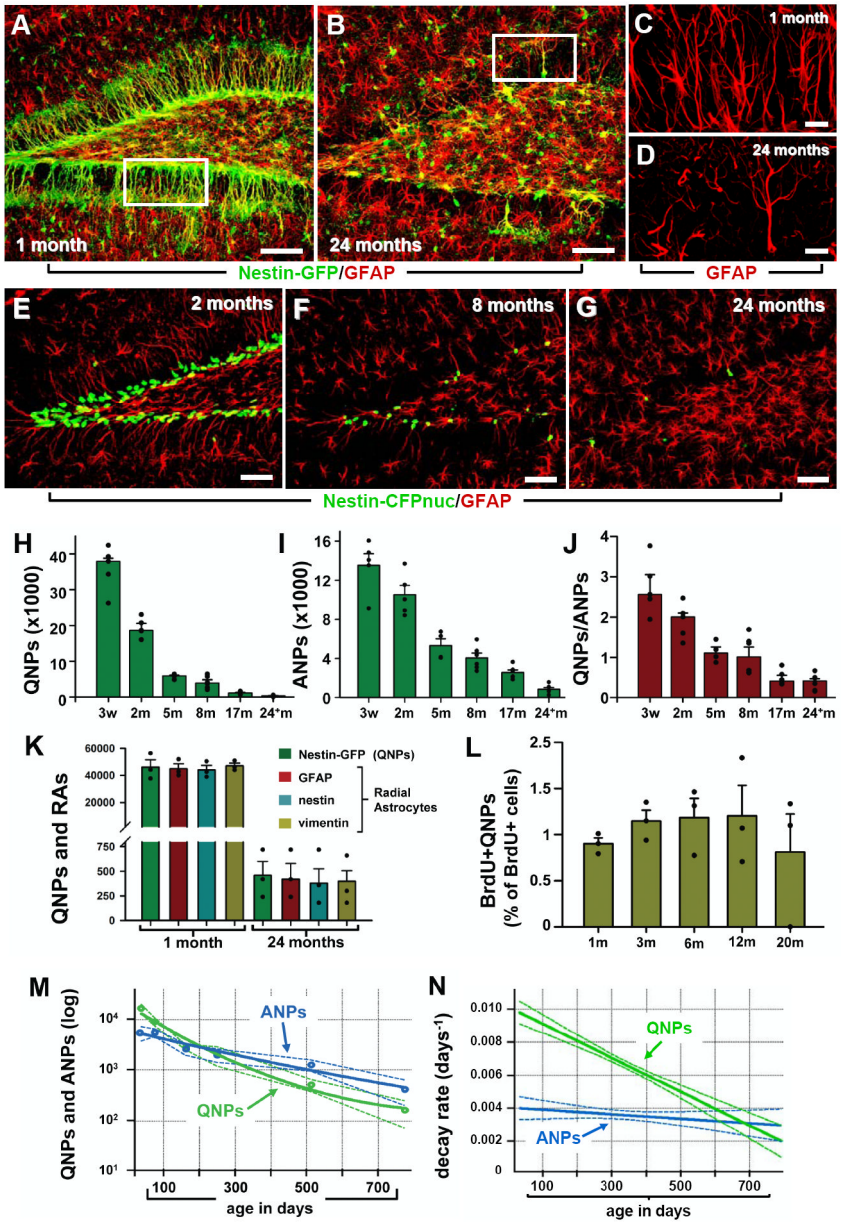

Fig. 3. Age-dependent decrease in the number of hippocampal stem and progenitor cells

(A-D) Nestin-GFP- and GFAP-positive cells in the DG of 1 month old **(A, C)** and 24 month old **(B, D)** Nestin-GFP mice. **C** and **D** correspond to the boxed regions in **A** and **B**, respectively, and show GFAP-positive radial astrocyte-like cells in 1 and 24 months old mice.

(E-G) QNP and ANP cells (green nuclei) in the DG of 2, 8, and 24 month old Nestin-CFPnuc mice. Note the increase in the number of GFAP-positive stellar astrocytes with age in **A, B, E-G**. Color channels are indicated. Scale bar is 50μm in **A, B, E-G**, and 25μm in **C, D**.

(H-J) Quantification of age-related changes in QNPs **(H)**, ANPs **(I)**, and the QNP/ANP ratio **(J)** in Nestin-CFPnuc animals (numbers, also presented in Table S2, are given as mean ±SEM; at least 4 animals per group). In this and other figures each animal is represented by a dot on the graph (such dots can overlap for close values).

(K) Quantification of Nestin-GFP QNPs and radial astrocyte-like cells (RAs) stained for GFAP, nestin, and vimentin in 1 and 24 months old Nestin-GFP animals.
(L) Percentage of BrdU-labeled QNPs among all QNP cells in Nestin-GFP mice of different ages after a single pulse of BrdU (150mg/kg, analyzed 24hr later).
(M, N) Polynomial fits of the QNP and ANP content **(M)** and the disappearance (decay) rates **(N)** of ANPs and QNPs. Dotted lines show a range corresponding to one standard deviation. The solid lines are interpolations.
See also Table S2.

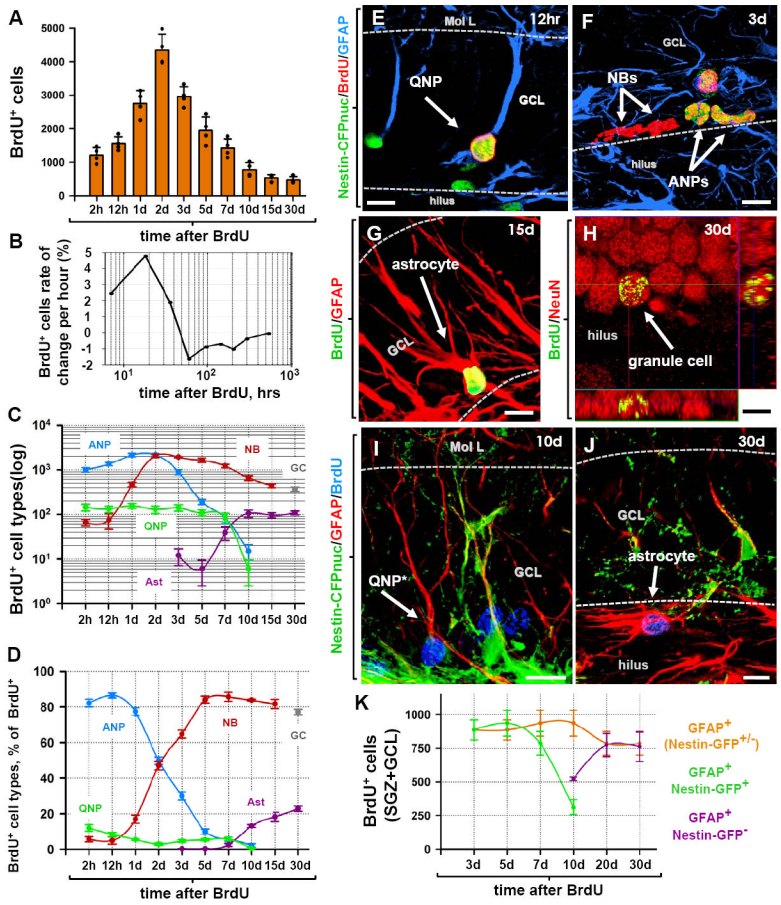

Fig. 4. The fate of dividing cells in the DG

(A) Time course of changes in the number of BrdU-positive cells after pulse labeling. 2 month old Nestin-CFPnuc mice (n=4 per time point) received a single injection of BrdU (150 mg/kg) and the number of BrdU-labeled cells in the DG was monitored over the course of 30 days.

(B) Rate of changes in the number of $BrdU^+$ cells, reflecting periods of active proliferation, rapid loss, and slower loss of the newborn cells.

(C, D) Time course of changes in defined classes of progenitors and mature cells in the DG of Nestin-CFPnuc mice. $BrdU^+$ cells were immunophenotyped to determine the numbers of labeled cells in defined classes. The results for QNPs, ANPs, NBs, mature neurons (granule cells, GC), and stellar astrocytes (Ast) are presented for the total number of cells in each class **(C)** and their fraction among total BrdU-labeled cells **(D)**. Note the logarithmic y scale in **C**.

(E-H). Differentiation of newborn cells in Nestin-CFPnuc mice. BrdU-labeled QNPs (12 hr after injection of BrdU, **E**), ANPs and NBs (3 days after injection, **F**), astrocytes (15 days after injection, **G**), and mature neurons (30 days after injection, **H**; shown with orthogonal projections). Color channels are indicated. Scale bar is 10μm.

(I-K) Pulse-chase experiment with Nestin-GFP mice. Nestin-GFP mice received a single injection of BrdU (150 mg/kg) and were sacrificed at different time points. At early time points after BrdU injection, all of the $BrdU^+GFAP^+$ cells also express Nestin-GFP and have QNP morphology. 10 days after BrdU injection, $BrdU^+GFAP^+$ cells lacking Nestin-GFP expression can be observed **(I)**. At this time the morphology of the $BrdU^+GFAP^+$ cells has already started to change, with branching of the apical $GFAP^+$ process. 30 days after BrdU

injection, none of the $BrdU^+GFAP^+$ cells express Nestin-GFP and their morphology resemble that of mature astrocytes **(J)**. Quantification of the time-dependent changes in the number of $BrdU^+GFAP^+$ cells (QNPs and astrocytes together), $BrdU^+GFAP^+GFP^+$ cells (QNPs), and $BrdU^+GFAP^+GFP^-$ cells (astrocytes) in the SGZ and GCL. Note that while the number of BrdU-labeled QNP cells declines, the number of BrdU-labeled $GFAP^+$ cells remains the same. Color channels are indicated. Scale bar is 10μm.

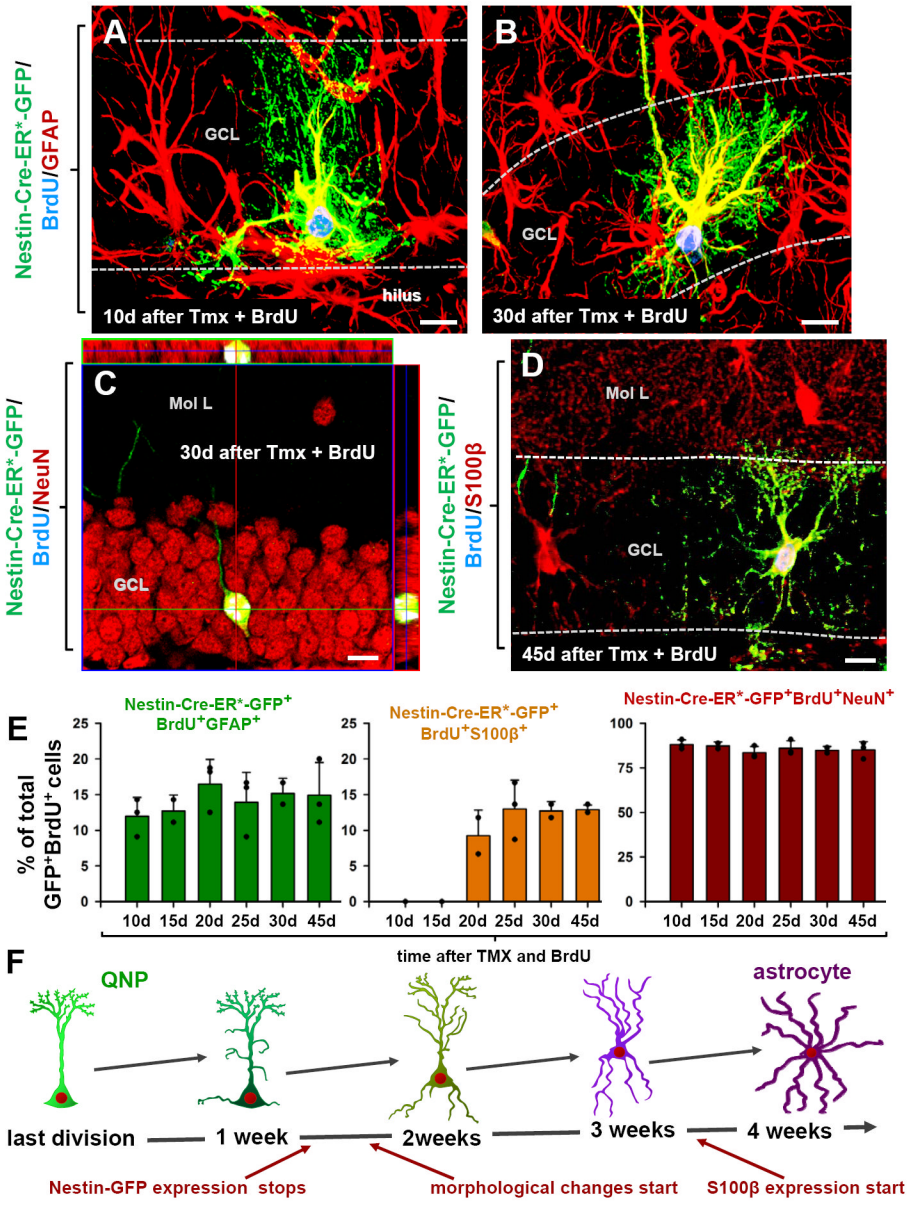

Fig. 5. QNPs undergo division-coupled astrocytic differentiation

(A-D) Recombination in Nestin-CreER/Z/EG mice (3-4 months old) was induced by tamoxifen treatment. Dividing cells were labeled by BrdU. 10 days after tamoxifen induction and BrdU labeling, GFP^+BrdU^+ QNPs change their morphology, branching their apical radial processes and extending basal cytoplasmic extensions with multiple ramifications **(A)**. 30 days later they extend processes from the soma, show characteristic star-shape morphology and extensive ramification of the branches and become indistinguishable from the surrounding stellar astrocytes **(B)**. $GFP^+BrdU^+NeuN^+$ granule neurons, detected 30 days after tamoxifen induction and BrdU injection; **(C;** shown with orthogonal projections). $GFP^+BrdU^+S100\beta^+$ mature astrocytes, detected 45 days after tamoxifen induction and BrdU injection **(D)**. Color channels are indicated. Bar is 10μm in **A-D**.

(E) Changes in $GFP^+BrdU^+GFAP^+$ cells (labeled QNPs and new astrocytes together), $GFP^+BrdU^+S100\beta^+$ cells (new mature astrocytes), and $GFP^+BrdU^+NeuN^+$ cells (new

neurons), as fraction of the total number of GFP^+BrdU^+ cells, after induction with tamoxifen and labeling with BrdU. Note that new mature astrocytes appear only 20 days after the induction and that the fraction of dividing QNPs and astrocytes does not undergo significant changes. Also note that the fractions of neurons and astrocytes among GFP^+BrdU^+ double-labeled cells is the same as for $BrdU^+$ single-labeled cells in Fig.4.

(F) Schematic representation, with a temporal scale, of the changes that QNP undergoes when becoming an astrocyte, with gradual appearance of the apical, basal, and somatic processes.

See also Figures S5 and S6.

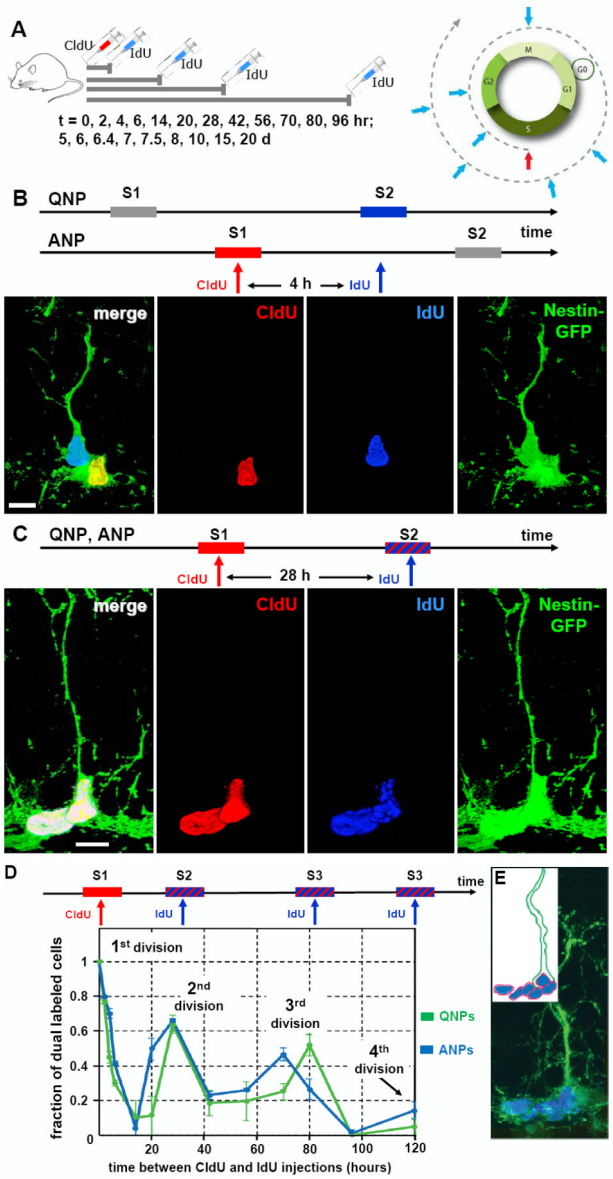

Fig. 6. Dynamics of QNP and ANP division in the DG

(A) General scheme of the double S-phase labeling protocol. Nestin-GFP mice (2 months old, n=3 per time point) received a single injection of CldU followed, at different time interval (t), by a single injection of IdU. Scheme on the right illustrates that a cell marked by CldU injection during the S phase is able to incorporate the second label (IdU) if it is injected during the same S phase but not later, during the G2, M, or G1 phases. However, the cell can become double-labeled if IdU is injected when the CldU-labeled cell again enters the S phase during the second, third, and subsequent rounds of division.

(B) An example of double S-phase labeling with the CldU and IdU injections separated by 4 hr. In this example the interval between label injections is not commensurate with the length of the cell cycle of the ANPs or QNPs, and CldU labels the S-phase of the ANP, but not of QNP, whereas IdU labels the S-phase of the QNP, but not of ANP. On the micrograph the nucleus of the ANP cells is labeled with CldU (red) and the nucleus of the QNP cells is labeled with IdU (blue); co-localization of CldU and GFP is yellow.

(C) An example of double S-phase labeling with the CdU and IdU injections separated by 28 hr. CldU labels the S-phase of the first division cycle and IdU labels the S-phase of the second cycle (stripped bar). The length of the cell cycle is commensurate with the interval between label injections and some cells have incorporated both labels. On the micrograph the nuclei of a QNP and an ANP cells (distinguished by the presence of a GFP-positive radial process) are labeled with CldU (red) and IdU (blue); triple co-localization is white. Scale bar is 10μm in **B, C**.

(D) Distinct cycles of division can be detected by determining the fraction of CldU/IdU double-labeled QNP and ANP cells at given time intervals. The length of the cell cycles can be determined from the position of the peaks and the length of the S phase can be determined from the slope of the decrease during the first S phase. Both QNPs (green) and ANPs (blue) divide several times in a close succession as suggested by the presence of several peaks in dual labeling (the first peak corresponding to the 0 hr time point); note that the first division also reflects the asymmetric division of the QNP that gives rise to an ANP.

(E) A cluster of dividing cells in the SGZ. Several BrdU-labeled ANPs are located next to a BrdU-labeled QNP after 2 hr labeling; such clusters should be observed if QNP, as well as ANPs, reenters the cell cycle but not if it becomes quiescent after giving birth to an ANP (note that this experiment was performed with 6 month old mice, in which progenitor cells undergo a larger number of divisions than in 2 months old animals and in which there are fewer dividing cells such that the clusters of dividing cells are well separated). Inset: schematic representation of the cells and their BrdU-labeled nuclei.

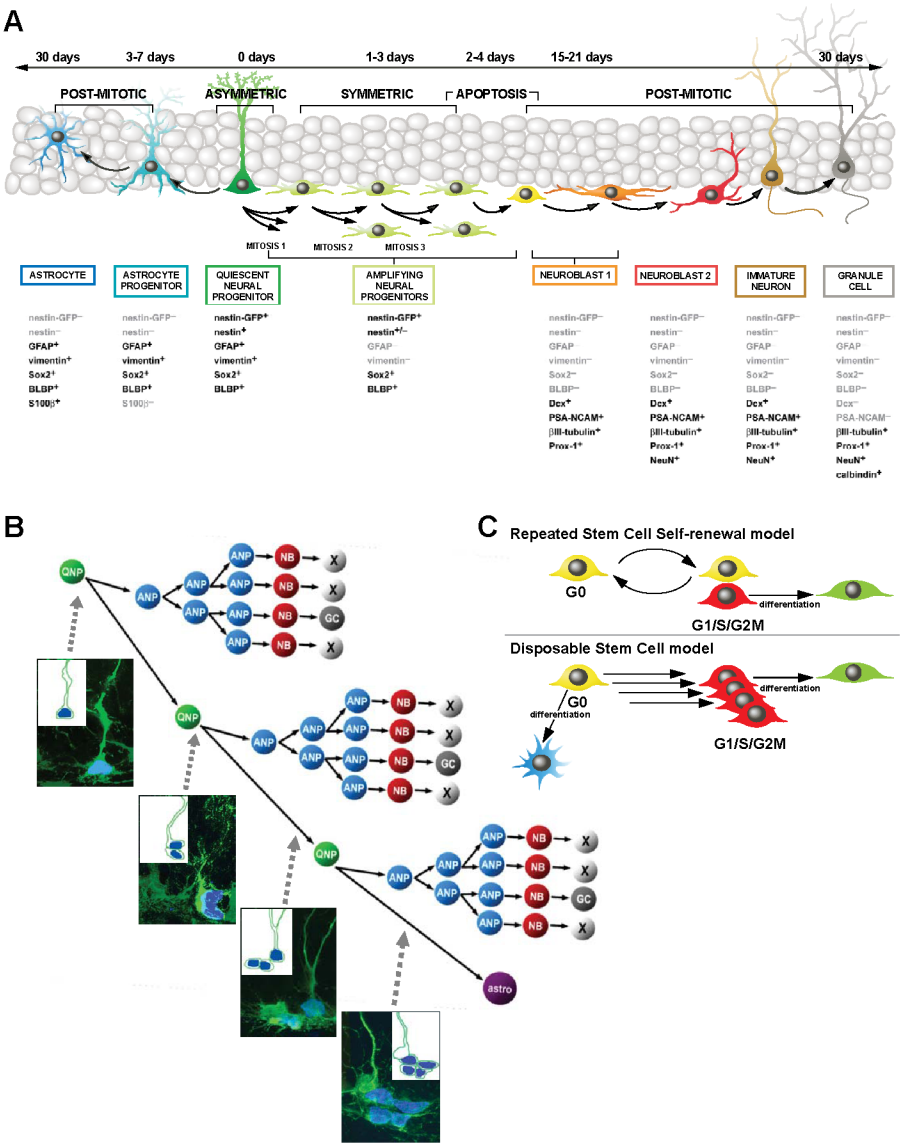

Fig. 7. A schematic summary of differentiation cascade in the DG

(A) A schematic summary of the neuronal and astrocytic differentiation cascade. QNPs generate, through ~3 several asymmetric divisions, the ANPs that, after ~2 rounds of symmetric divisions, exit the cell cycle and become NB1 cells. NB1 cells mature into NB2 and then into INs and differentiated mature neurons; this is accompanied by a massive loss of newborn cells. After a rapid succession of several divisions, QNPs exit the cell cycle and start acquiring the astrocytic morphology. The estimated number of division cycles is presented for a young adult (2-3 months old) mouse and is expected to be different at other ages. Time intervals of the major steps of the cascade are indicated.

(B) A scheme of divisions and death of stem cells and their progeny in the DG. Micrographs correspond to the predicted combinations of BrdU-labeled cells after short-term labeling; from top to bottom – first S phase of a QNP; second S phase of a QNP and the first S phase of the daughter ANP; third S phase of a QNP and second S phase of the daughter ANPs; QNP exiting the string of division (unlabeled) and progeny ANPs in the third S phase. Insets: schematic representation of the cells and their BrdU-labeled nuclei.

(C) In the conventional “repeated stem cell self-renewal” model, a quiescent stem cell is activated, undergoes an asymmetric division, produces a progeny that eventually differentiates (in this case into a neuron), and returns to the quiescent state to be activated again several times until the death of this stem cell or of the organism. In the “disposable stem cell” model, a stem cell is quiescent for the entire postnatal life, is activated, undergoes several rapid asymmetric divisions producing progeny and quits the pool of stem cells by differentiation (in this case into an astrocyte).